Introduction of misfit dislocations into strained-layer GaAs/In$_x$Ga$_{1-x}$As/GaAs heterostructures by mechanical bending

Journal Item

For guidance on citations see FAQs.

oro.open.ac.uk

Introduction of misfit dislocations into strained-layer GaAs/In$_x$Ga$_{1−x}$As/GaAs heterostructures by mechanical bending

X. W. Liu[1] and A. A. Hopgood[1,2] [*]
[1]*University of Portsmouth, Faculty of Technology, Portland Building, Portland Street, Portsmouth, PO1 3AH, United Kingdom*

[2]*Open University, Faculty of Science, Technology, Engineering, and Mathematics, Walton Hall, Milton Keynes, MK7 6AA, United Kingdom*

[*] Corresponding author:
adrian.hopgood@port.ac.uk

ABSTRACT:

The stability of strained-layer heterostructure lasers can be assessed by their response to stimuli for the introduction of dislocations. Three-point bending at elevated temperatures has been applied to GaAs/In$_x$Ga$_{1-x}$As/GaAs heterostructures to apply such a thermomechanical stimulus. In each case, the middle-layer thickness was below the critical thickness predicted by Matthews-Blakeslee model, so that the pre-test structures were fully strained with no observed misfit dislocations. The tensile stress of 46.4 MPa produced during the tests resulted in the formation of 60˚ misfit dislocations whose configurations changed according to the alignment of the bending axis. For bending in the [110] orientation, the misfit dislocations formed parallel to each other and to the bending axis. For [100] bending, they formed an orthogonal pattern with each dislocation at 45˚ to the bending axis. In each case, these misfit dislocations caused relaxation of the strained-layer structures, even though the unloaded structures had been considered thermodynamically stable and the test temperatures were lower than those used during the original fabrication of the structures. These findings challenge existing assumptions of strained-layer stability and have implications for the design of lasers intended to be "buried and forgotten" in optical telecommunications.

1   INTRODUCTION

The long-term reliability of semiconductor lasers is vital to their utility in the telecommunications industry [1], yet strain is often deliberately introduced in the active layer in order to tailor the laser's characteristics and performance [2]. A key factor in that reliability is the stability of the strained layer and, specifically, the propensity to form misfit dislocations at the strained-layer interfaces [3]. Recent studies have shown the importance of strain on the optoelectronic performance of lasing devices [4, 5], but this study focuses on their materials properties.

The particular heterostructures discussed here comprise a compressively strained $In_xGa_{1-x}As$ quantum well surrounded by GaAs layers. These quantum wells are the basis of telecommunications lasers operating at 980nm, a longer wavelength than the equivalent unstrained structures. One of their potential uses is to pump erbium-doped optical fiber amplifiers, but reliability is vital. Since telecommunications companies expect a 20-year lifetime or longer, the gradual degradation of strained-layer lasers has long been a cause for concern [6]. Any experiments that test the stability of the strained-layer in more manageable laboratory timescale are therefore to be welcomed.

The current work has investigated the stability of the strained-layer interfaces to mechanical bending at elevated temperatures. These thermomechanical tests are complementary to previous studies that have shown that misfit dislocations can be induced by post-fabrication thermal processing in both strained [7] and partially relaxed [8] structures. Although mechanical bending is not a normal environmental hazard, it can nevertheless offer a useful method for providing an additional insight into the stability of the structure.

The atoms at the interface of a heterostructure are subjected to the two competing periodicities of the crystal structures at either side of the interface. The misfit between epilayer and substrate structures may be accommodated by misfit dislocations, or misfit strain, or both [9]. If the strained layer is thin enough, the Matthews-Blakeslee model [10] predicts that there is a critical

thickness for a given misfit, below which the misfit will be accommodated entirely by strain of the epilayer without the formation of any misfit dislocations. Some researchers have observed empirically higher critical thicknesses [11], while others [12] have found the Matthews-Blakeslee criterion to be an accurate predictor of the onset of the first few misfit dislocations. More recent studies in GaAs/GaAs$_{1-x}$Sb$_x$/GaAs heterostructures have shown the evolution of the misfit dislocations as the thickness of the strained layer increases [13]. De la Mata et al. [14] have used atomic resolution high angle annular dark field scanning transmission electron microscopy with geometrical phase analyses and computer simulations, to establish in detail the relaxation mechanisms in related structures. While discussion continues about the validity of the models of dislocation formation, the approach taken in this article is based on physical rather than computer-based experimentation.

A strained-layer structure is subjected to an unusual loading condition, that of constant biaxial deformation, where the strain relief is proportional to the density of misfit dislocations [15]. Dodson and Tsao [15] developed a model for the relaxation of an initially coherent metastable strained layer using standard descriptions of dislocation dynamics and relaxation via plastic flow. Some years later, Zaumseil et al [16] published the first experimental study of the relaxation and diffusion behavior of pseudomorphically grown Si$_{1-x}$Ge$_x$ layers under high hydrostatic pressure at room temperature and at high temperatures. They demonstrated that, after high pressure (between 10 MPa and 2.5 GPa) treatment at room temperature, the samples show no structural changes compared with the as-grown state. In contrast, annealing at 900–950˚C under high pressure was shown to cause both a large increase in relaxation and enhancement of the Si-Ge interdiffusion. Consequently, the density of misfit dislocations was observed to be much higher in the high-pressure annealed sample.

An applied stress produced by mechanical bending has been used historically to investigate dislocations in semiconductor materials [17–22]. More recent studies have analyzed bending induced by the stresses created in fabrication [23, 24]. Other mechanical tests have included

indentation hardness and compressive deformation [25]. The aim of this paper is to present an investigation into whether relaxation of GaAs/In$_x$Ga$_{1-x}$As/GaAs heterostructures can be induced through the formation of misfit dislocations during three-point bending at elevated temperatures.

2 EXPERIMENTAL DETAILS

All the structures considered here comprise a single strained layer of In$_x$Ga$_{1-x}$As of thickness h between surrounding layers of GaAs. The specimens were grown by molecular beam epitaxy (MBE). A 50 nm AlAs layer was first grown epitaxially on a 0.5 mm thickness GaAs (001) substrate, followed by a 200 nm layer of GaAs, a layer of In$_x$Ga$_{1-x}$As of thickness h, and a second 200 nm layer of GaAs. The growth temperature was 800K for the In$_x$Ga$_{1-x}$As layer and 870K for other layers. The growth rate was 1μm/hour. The composition and layer thickness were calibrated by x-ray diffraction. The surface morphology was monitored during growth by reflection high-energy electron diffraction (RHEED).

Three types of specimen were considered: $x = 0.15$ with $h = 6$ nm, $x = 0.15$ with $h = 15$ nm, and $x = 0.20$ with $h = 4$ nm. In each case h was below the critical value, H_c, predicted by the Matthews–Blakeslee model [10] for misfit dislocation formation in a double heterostructure (15nm for x=0.20, and 21nm for x=0.15). In the cases of $x = 0.15$ with $h = 6$ nm and $x = 0.20$ with $h = 4$ nm, the strained layer thickness was also below the critical thickness, h_c, predicted for a single layer of In$_x$Ga$_{1-x}$As on GaAs (7nm for x=2.0, and 9nm for x=1.5). In these two cases, no misfit dislocations would have been expected. In the sample with h falling between h_c and H_c, some misfit dislocations might have been expected since, during growth, the specimen would have been a single heterostructure before the second GaAs layer was added. In fact, no misfit dislocations, and hence no relaxation, were observed in any of the structures prior to the bending tests. The equation for H_c, from which h_c is also derived, is presented in [9].

1 mm × 3 mm specimens were obtained by cleaving along <110> or <100>. Three-point bending tests were carried out on a rig specifically designed for this research, illustrated in Fig. 1.

The short (1mm) edge was parallel to the bending axis and the long edge (3 mm) parallel to the neutral axis. As the strained layers faced downward and were much thinner than their substrate, the bending moment subjected them to a tensile stress. A fixed load W of 2.864 N produced a maximum tensile stress σ_{max} of 46.4 MPa on the specimen surface, as derived from the standard three-point bending equation [26]:

$$\sigma_{max} = \frac{My}{I} \tag{1}$$

where M is the bending moment, y is the distance from the surface to the neutral axis, and I is the second moment of area. The bending moment is $WL/4$, where L is the separation of the fulcrums (2.7 mm), and I for a rectangular geometry of thickness d and breadth b is $bd^3/12$. Bending tests at temperatures up to 730 K were carried out within a Carbolite furnace. The target temperature was maintained for 1s, after which the furnace door was opened, and the sample cooled in air inside the furnace. Tests were performed with the bending axis parallel to [110] (as in Fig. 1) and parallel to [100] for each of the three structures. A variety of temperatures were tried, and we present here a selection of micrographs that show an observable effect.
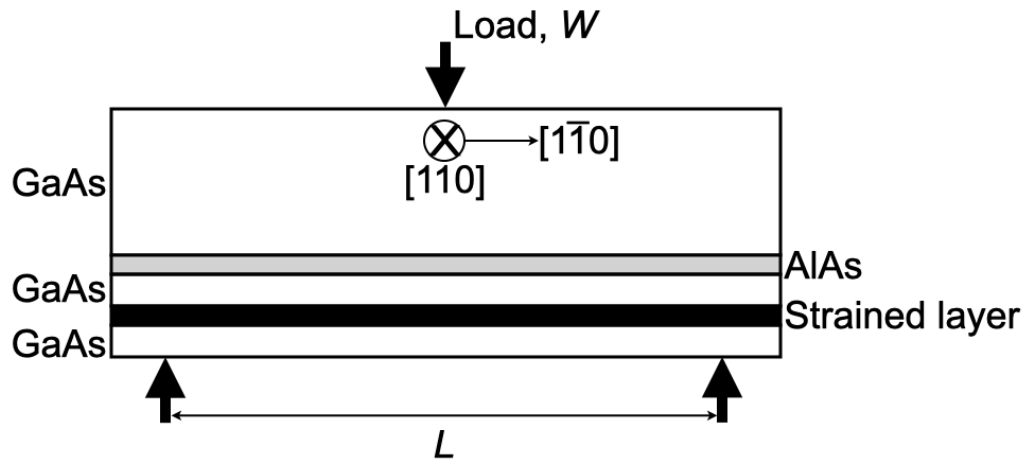

Fig. 1. Three-point bending in [110] orientation. The 1mm side of the specimen was parallel to the bending axis, normal to the plane of the diagram.

The use of cathodoluminescence (CL) imaging on a JEOL JSM-820 scanning electron microscope (SEM) allowed dislocations to be examined at low magnification in a bulk specimen, thereby avoiding the risk of the dislocation configuration being altered by specimen preparation. Film specimens for transmission electron microscope (TEM) observation were prepared using the epitaxial lift-off (ELO) technique [12]. This technique involves etching away a sacrificial AlAs layer in order to release the heterostructures from the substrate. TEM observation was on a JEOL 2000FX operated at 200 kV. Cross-sectional TEM inspection allowed the thickness of the strained layer to be confirmed [12, 23]. CL and TEM imaging were used to confirm that no damage had occurred during processing. All TEM micrographs presented in this article were taken from (001) planar thin-film samples. All CL and TEM micrographs are plan-view, looking down the [001] direction, tilted depending on the **g** vector in the case of the TEM images.

3   RESULTS

The observed dislocation structures following bending tests in the [110] and [100] orientations are presented in this section. Due to the bending configuration described in Section 2, the principal effect on the strained-layer structure is to apply tension. The motivation for the study was to investigate the stability of these laser structures to the formation of dislocations under any form of stimulus.

3.1   [110] bending tests

Fig. 2 shows successive CL images of a GaAs/In$_{0.15}$Ga$_{0.85}$As/GaAs double heterostructure with h = 15 nm after consecutive [110] bending tests. It shows the development of dislocations from a few short ones at 670 K in Fig. 2(a), to longer ones at 690 K in Fig. 2(b), through to a substantial increase in length and density at 710 K in Fig. 2(c). Dislocations A, B, C, and D in Fig. 2(a) were not elongated further when the temperature increased by 20 K as shown in Fig. 2(b) although some new and longer dislocations appeared. The approximately horizontal lines are artifacts caused by scratches.
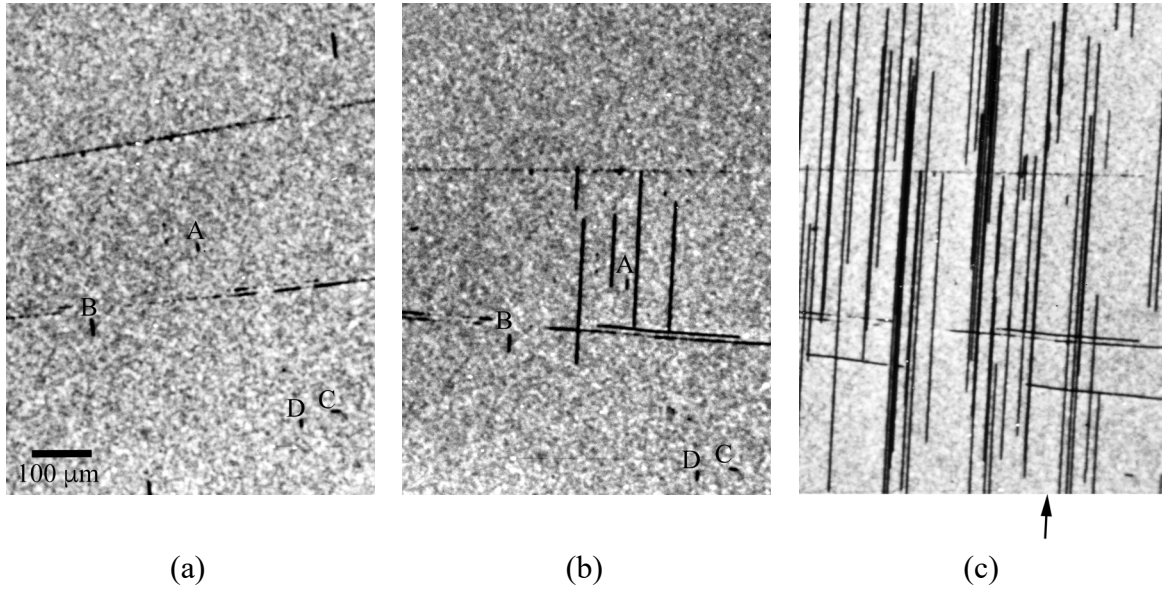
Fig. 2. Successive CL [001] plan-view images of a GaAs/In$_{0.15}$Ga$_{0.85}$As/GaAs (h = 15 nm) heterostructure after [110] bending at (a) 670 K, (b) 690 K, and (c) 710 K. The magnification is the same for all three images and the orientations similar; the arrow indicates the direction of the bending axis.
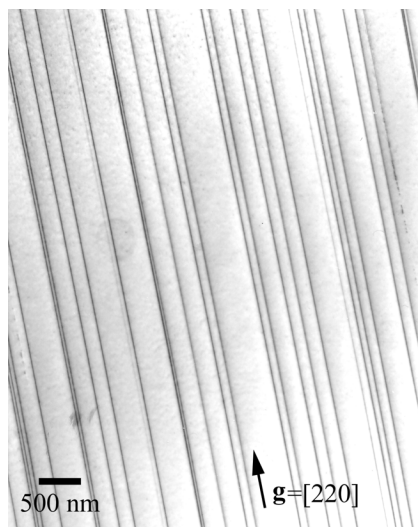

Fig. 3. TEM [001] plan-view image of dislocations caused by [110] bending in GaAs/In$_{0.15}$Ga$_{0.85}$As(h = 15 nm)/GaAs.

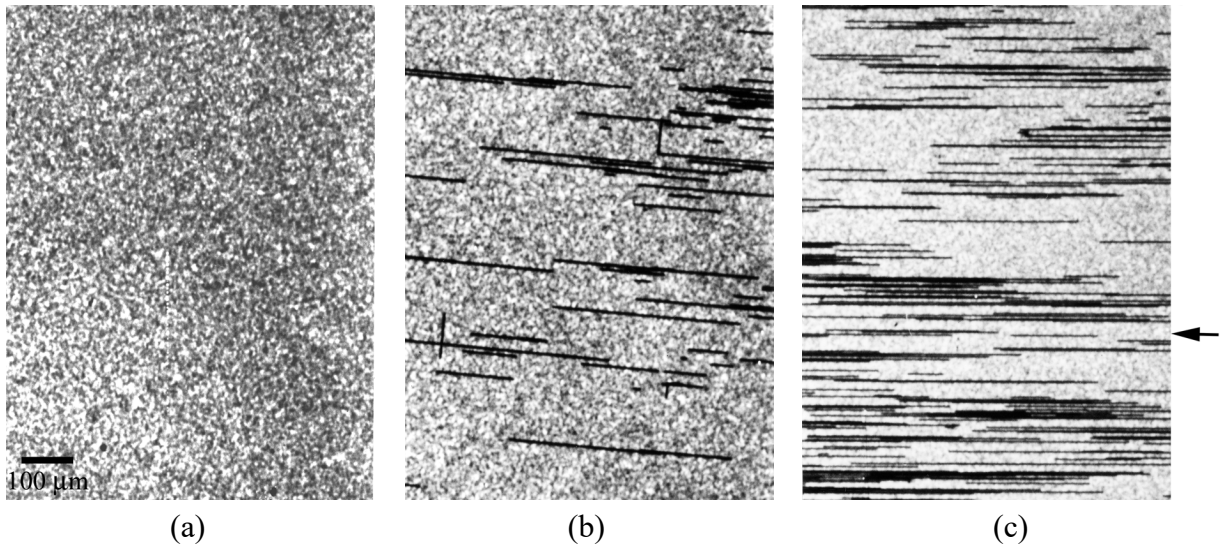(a)   (b)   (c)

Fig. 4. CL [001] plan-view images of GaAs/$In_{0.15}Ga_{0.85}As$/GaAs ($h = 6$ nm) specimens after [110] bending at (a) 620 K, (b) 670 K, and (c) 690 K. The magnification is the same for all three images and the orientations similar; the arrow indicates the direction of the bending axis.
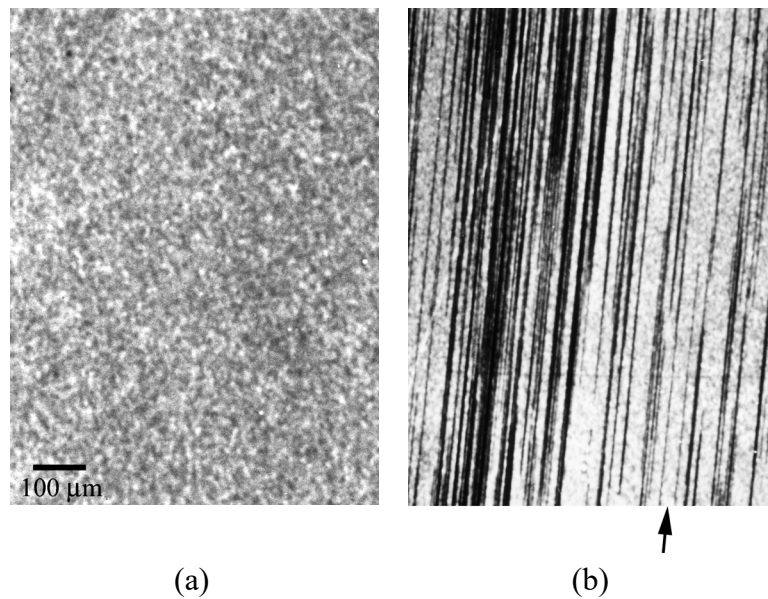

(a)   (b)

Fig. 5. CL [001] plan-view images of dislocations in a specimen of $x = 0.2$, $h = 4$ nm after [110] bending at (a) 690 K and (b) 710 K. The magnification is the same for both images and the orientations similar; the arrow indicates the direction of the bending axis.

The dislocations revealed by CL imaging appeared as black lines parallel to the short (1mm) edge of the specimens. From the geometry of the bending rig, it can be inferred that the dislocations form parallel to the [110] bending axis, as indicated on the CL micrographs. This inference has been confirmed by TEM imaging (Fig. 3), which has shown that the dislocations formed during these tests have identical characteristics to 60˚ misfit dislocations oriented parallel to [110]. The same results were found for the dislocations caused by [110] bending in the other double heterostructures considered here, i.e. GaAs/$In_{0.15}Ga_{0.85}As$/GaAs with $h = 6$ mm (Fig. 4) and GaAs/$In_{0.20}Ga_{0.80}As$/GaAs with $h = 4$ mm (Fig 5). Figs. 4(a) and 5(a) are CL images that show no evidence of dislocation formation.

3.2   [100] bending

The effects of an applied tensile stress on the formation of dislocations in a compressive strained layer can be demonstrated by [100] bending followed by CL imaging, as shown in Fig. 6. The specimen shown is GaAs/$In_{0.15}Ga_{0.85}As$/GaAs with $h = 15$ nm after bending at 710K. A boundary, indicated by arrows, can be seen between the regions of high and low dislocation density. This boundary coincides with the position of one of the two outer loading axes for three-point bending. Outside the two outer loading axes, there was no applied tensile stress. Between the axes, the dislocation density is greatest at the center, where the bending moment is greatest [27] (Fig. 7).
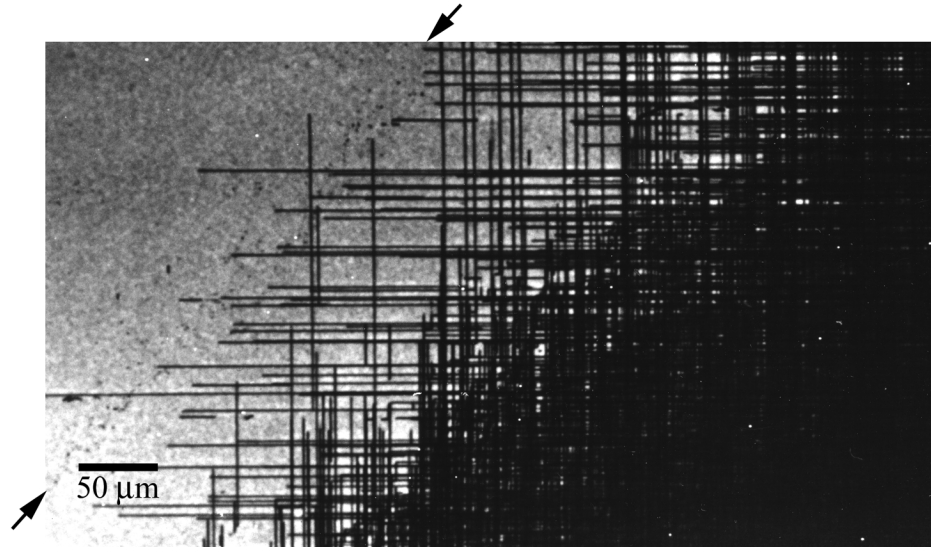
Fig. 6. CL [001] plan-view image showing dislocated and non-dislocated regions caused by [100] bending in GaAs/In$_{0.15}$Ga$_{0.85}$As/GaAs (h = 15 nm) at 710K. The two arrows mark the delineation of the loaded area.

The TEM image in Fig. 8 shows that dislocations caused by [100] bending form a network of orthogonal 60° dislocations similar to those seen in as-grown relaxed heterostructures where the critical thickness has been exceeded [4]. Unlike [110] bending, the dislocations are aligned at 45° to the bending axis, in the <110> direction. As well as the dislocations aligned along [110] or [$\bar{1}\bar{1}$0], which are the same as those formed during [110] bending, there are also dislocations along [$\bar{1}$10] and [1$\bar{1}$0]. This difference is because the tensile stress due to [110] bending acts on the first slip system only, whereas the tensile stress has equal components in both slip systems in the case of [100] bending.

Similar observations were made following [100] bending of the other double heterostructures considered here. For comparison, Fig. 9 shows dislocations caused by [100] bending under the same experimental parameters in a GaAs specimen. These dislocations are short and irregular, demonstrating that the dislocation structures observed in the other micrographs are caused by the heterostructures and do not simply arise from crystal geometry.
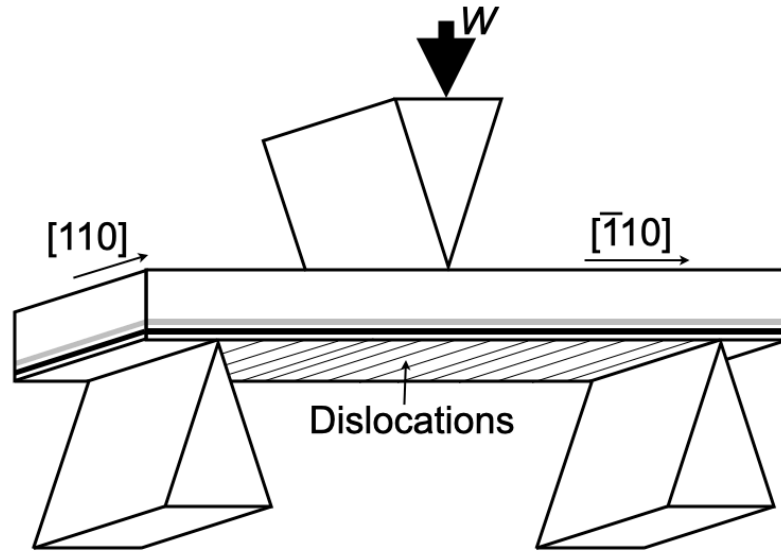
(a)
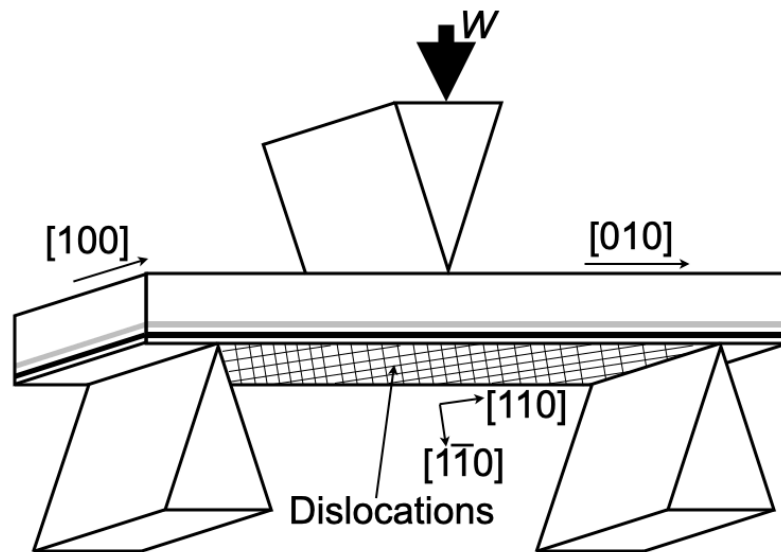
(b)

Fig. 7. Area of dislocation formation in a strained-layer structure under three-point bending along (a) [110] and (b) [100].
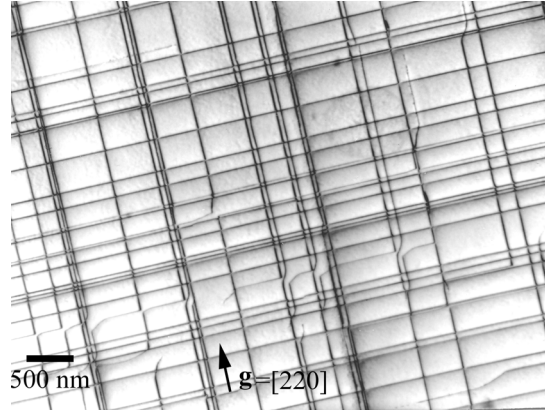
Fig. 8. TEM [001] plan-view image of dislocations caused by [100] bending in GaAs/In$_{0.15}$Ga$_{0.85}$As(h = 15 nm)/GaAs at 710K.
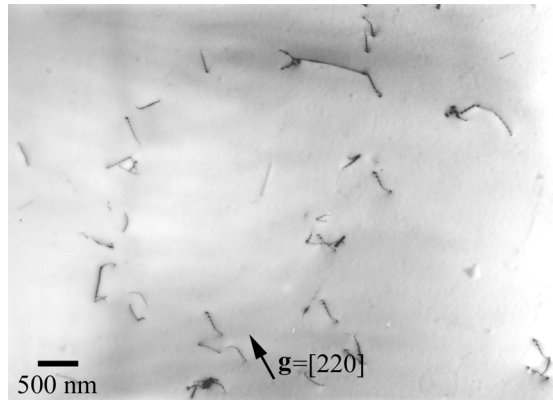

Fig. 9. TEM [001] plan-view image of dislocations caused by [100] bending in GaAs at 710K.

4   DISCUSSION

It has been shown that misfit dislocations can be introduced by bending strained-layer heterostructures, resulting in relaxation of the structure. Very few threading segments of misfit dislocations can be found in the TEM images in Figs. 3 and 8. This sparsity implies that the dislocations formed during the bending tests are relatively long. They can grow extensively without meeting a crystal surface because they are confined to move along (001) interfaces, parallel to the surfaces of the specimens, in the direction of the intersections of the {111} slip planes and (001) interfaces. This observation provides further evidence that the dislocations that
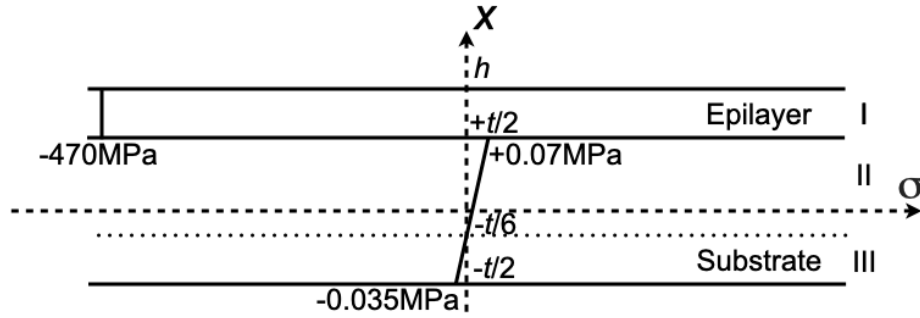
Fig. 10. Stress distribution in a strained-layer structure with the thickness of substrate $t = 0.4$ mm and strained layer $h = 15$ nm.

4.1 Distribution of misfit stress in strained-layer structures

The relaxation of a strained-layer structure is strongly dependent on the local stress field and it is therefore important to understand the stress distribution [28]. The equilibrium stress state of a strained-layer system can be obtained by balancing the forces and moments. Assuming that Poisson's ratio v is the same for the film and the substrate, and that the origin of the x axis is at half the thickness of the substrate, the stress distribution σ for a structure as illustrated in Fig. 10 is given by [28, 29]:

$$\sigma_s(x) = \pm \frac{G_f \varepsilon}{1-v}\left(\frac{h}{t} + 6\frac{h}{t^2}x\right) \text{ for } x \in \left[-\frac{t}{2}, \frac{t}{2}\right] \tag{2}$$

$$\sigma_f(x) = \pm \frac{G_f \varepsilon}{1-v}\left[1 - 6\frac{G_f h}{G_s t^2}\right]\left(x - \frac{h+t}{2}\right) \text{ for } x \in \left[\frac{t}{2}, \frac{t}{2} + h\right] \tag{3}$$

where t and h are the thicknesses of substrate and film respectively, ε is the elastic strain, G is the shear modulus, and s stands for substrate and f for film.

The surface of the substrate adjacent to a compressed strained layer is subjected to tension, and the opposite surface of the substrate is subject to compression. The plane within the substrate where the stress is zero is termed the neutral plane. The coordinate of the neutral plane in the structure shown in Fig. 10 is $-t/6$ [28]. In a strained-layer structure with $t = 0.4$ mm and $h = 15$ nm, Equation 1 yields $\sigma_s = 0.07$ MPa for the surface of substrate at $t = +0.2$ mm and 0.035 MPa at $t = -0.2$ mm. Equation 2 shows the stress within the strained layer to be almost uniform at -470 MPa.

Three distinct stress regions can be delineated. Region I is the strained layer, where the stress is compressive for the structures considered here and the stress level is the highest. Regions II and III are respectively the tensile and compressive parts of the substrate, separated by the neutral plane. The level of the stress in these regions is much lower than that in Region I. The misfit stress in a strained-layer structure is mainly concentrated within the strained layer and the substrate can be considered to remain unaffected so long as it is thick enough [23, 28].

The strained-layer structures investigated here include a GaAs capping layer that is about 10 times the thickness of the strained layer. It is sufficiently thick to produce a stress distribution at the capping-layer/strained-layer interface similar to that at the substrate/strained-layer interface.

An externally applied stress of 46.4 MPa is low compared with the stress of 470 MPa within the strained layer. However, it is sufficient to change the distribution of the local stress field near the interface because the maximum stress at the substrate side is only 0.07 MPa. Therefore, an externally applied stress can be expected to affect the mechanical stability of the interface and the behavior of misfit dislocations.

4.2 Mechanical stability of interface

For a compressive strained-layer structure, the lattice of the strained layer is constrained by that of the substrate, as illustrated in Fig. 11. An applied tensile stress helps the strained layer lattice to recover its normal state but increases the tensile stress on the substrate.
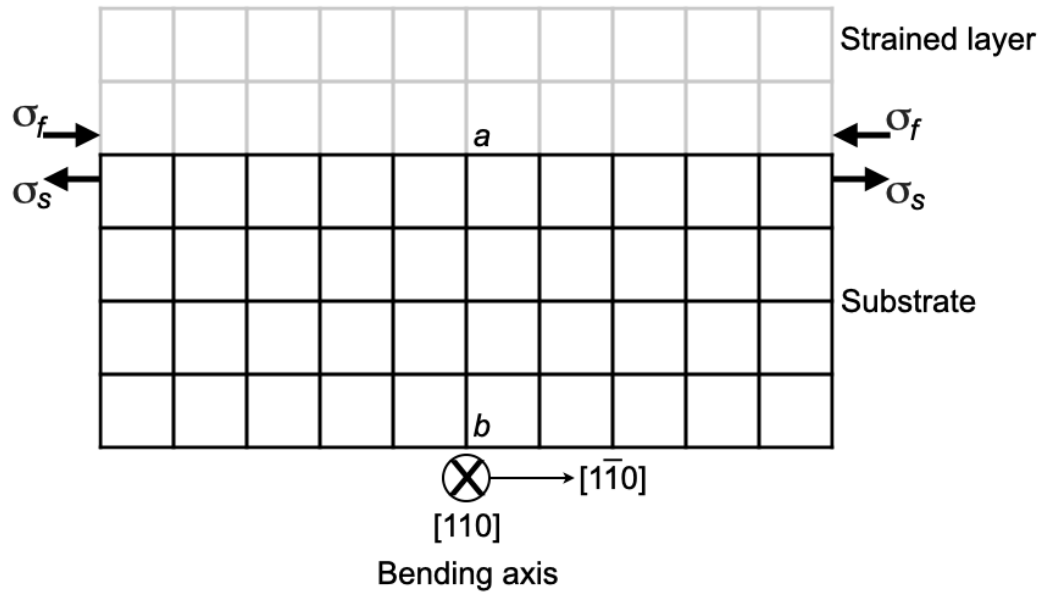
Fig. 11. Stresses σ_f and σ_s due to lattice mismatch on a compressively strained layer and the substrate respectively.

Nadgornyi [30] has reported that the dislocation velocity in GaAs under an applied stress of 10 MPa at 670–770 K is higher than that at 470 K by a factor of approx. 10^5. This observation indicates that dislocation behavior in GaAs is highly temperature-dependent. An external stress of this order applied at a temperature above 670 K can be sufficient to cause deformation-producing dislocations [19] and even to stimulate dislocation activation in dislocation-free materials, using existing microdefects as dislocation sources [15]. The development of dislocations shown in Figs. 2, 3, 4, 5, 6, and 8 provides evidence that crystal lattices have become unstable during the bending tests and that mechanisms of deformation are operating through the generation and motion of dislocations [31, 32].

The force exerted on dislocations by misfit stress plays an important role on the generation and motion of dislocations [32, 33, 34]. Consider the [110] bending shown in Fig. 11. The externally applied stress acts to expand the lattices in the same direction as the misfit stress. If plastic deformation of the lattices occurs, i.e. dislocations are formed, the normal to the resultant

half-planes will be parallel to the direction of expansion, i.e. parallel to the direction of the applied stress. The position of the half-planes will correspond with the *a–b* plane in Fig. 11. If the *a–b* planes include the direction of slip, dislocations will propagate along these planes.

However, a strained-layer system influences the dislocation motion in favor of the relaxation of its own structure. For a strained-layer system with a face-centered cubic or diamond structure, the slip planes combined with (001)-oriented strained interfaces make the <110> directions in (001) planes the most energetically favorable slip system [35, 36]. The misfit stress acts on the dislocations and constrains them to move only in the <110> / (001) slip system. The dislocations produced in this way adopt the form of misfit dislocations. Thus, the directions of dislocation movement in a bending test are confined within a plane in a strained-layer system, i.e. the <110> / (001) intersections, rather than exhibiting the volumetric freedom observed in unstrained structures. As a result of the applied stress combined with the misfit stress, dislocations will appear in a GaAs/In$_x$Ga$_{1-x}$As/GaAs specimen subjected to [110] bending as straight lines along interfaces whose line directions are parallel to the bending axis. These dislocations result in both the relaxation of the strained-layer structure and the deformation of the crystal.

These combined effects of applied stress together with misfit stress on strained-layer structures can be verified by comparison with unstrained GaAs. With the same applied bending stress, the dislocations formed in GaAs are irregular and disordered because there is no misfit stress in the structure to constrict the dislocation activity.

For [100] bending, because [100] is not the direction of slip, the effective stress is the component of applied stress in the slip directions, [110] and [1$\bar{1}$0]. Consequently, [100] bending of GaAs/In$_x$Ga$_{1-x}$As/GaAs causes the formation of a network of orthogonal dislocations oriented along [110] and [1$\bar{1}$0].
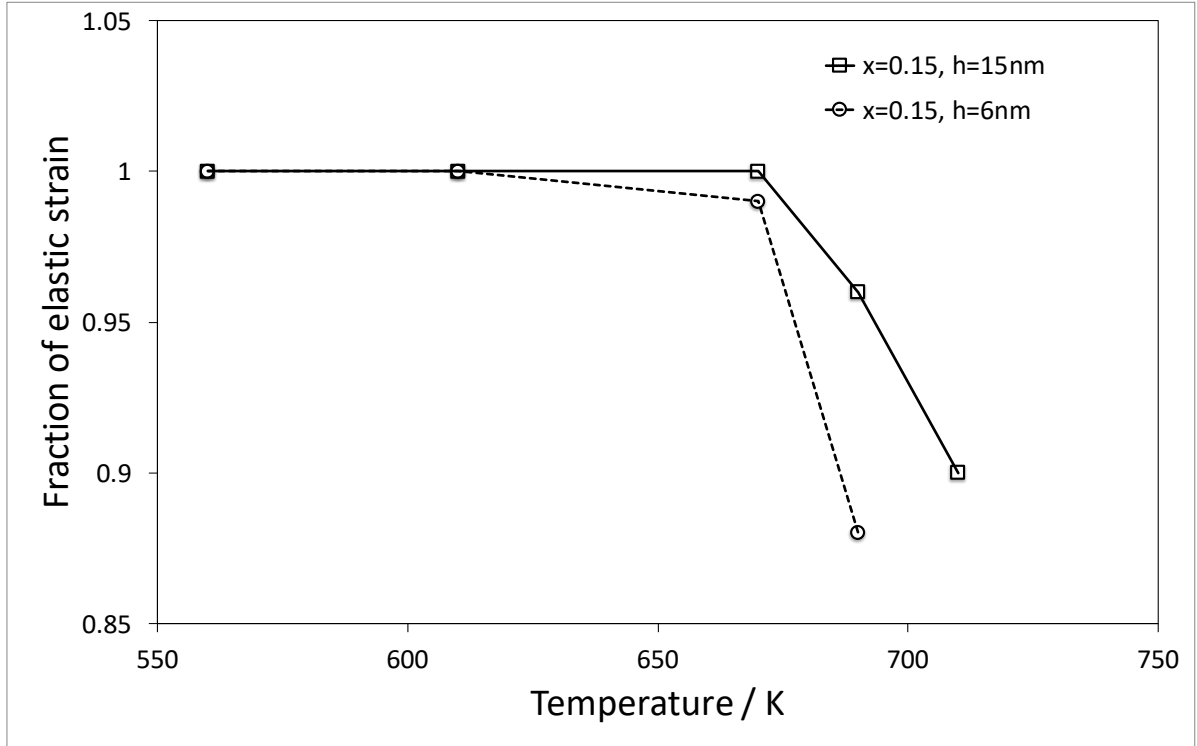
Fig. 12. Reduction in elastic strain caused by the formation of misfit dislocations during [110] bending tests. Data points for $h = 15$ nm: (560, 1) (610, 1) (670, 1) (690, 0.96) (710, 0.90); for $h = 6$ nm: (560, 1) (610, 1) (670, 0.99) (690, 0.88).

4.3 Relaxation through the formation of misfit dislocations

The appearance of misfit dislocations indicates the loss of coherence between a strained layer and its substrate. The misfit must be accommodated by elastic strain ε and plastic strain δ caused by misfit dislocations, so:

$$f = \frac{a_s - a_0}{a_s} = \varepsilon + \delta \qquad (3)$$

where a_S and a_O are the lattice parameters of the substrate and overlayer respectively. Because misfit dislocations exist at the interface, δ is non-zero and can be estimated from the misfit dislocation spacing S,

$$\delta = \frac{b_e}{S} \qquad (4)$$

where b_e is the interface-plane component of the Burgers vector in the direction of spacing S.

The plastic strain δ is a measure of relaxation caused by the formation of misfit dislocations. From Equation (1), the reduction in elastic strain in a strained-layer structure due to the formation of misfit dislocations is $\varepsilon = f - \delta$. If we assume the proportions of elastic and plastic strain to be 100% and 0% respectively before any tests, Fig. 12 shows the changes in these proportions caused by the formation of misfit dislocations during a [110] bending test. These changes only occurred perpendicular to the line directions of dislocations.

It can be seen in Fig. 12 that 10%–12% of misfit strain is relaxed by the formation of misfit dislocations. Although these unloaded specimens can be classified as thermodynamically stable structures according to the theoretical model [6], relaxation caused by an applied stress occurred even at temperatures 670K – 710K, which are lower than the fabrication temperature of 870K.

5   CONCLUSIONS

It has been shown that an applied stress can bring about relaxation in a strained-layer structure. The configurations of dislocations formed in GaAs/In$_x$Ga$_{1-x}$As/GaAs (with $h < h_c$ or $h_c < h < H_c$) during bending tests demonstrate the combined effects of misfit stress and applied stress on the formation of misfit dislocations. Under an applied stress, misfit dislocations are produced as a result of both relaxation of the strained-layer structure and deformation of the crystal. Because of the addition of the mechanism of mechanical deformation, the strained-layer thickness at which the relaxation will occur becomes smaller, even at temperatures lower than when structures were built up during fabrication.

Although this study has focused on a specific strained-layer system, the findings could have implications for a variety of other systems, e.g. [4, 5]. As the current work is based on empirical

evidence and theoretical analysis, finite-element modelling (FEM) of the stress distributions and dislocation interactions is a suggestion for future work.

ACKNOWLEDGEMENTS

DATA AVAILABILITY STATEMENT

The data that support the findings of this study are available within the article.

REFERENCES

1. R. Herrick and O. Ueda (eds), *Reliability of Semiconductor Lasers and Optoelectronic Devices*, Elsevier, in press (2021).

2. S. Sweeney, T. Eales, and A. Adams, *J. Appl. Phys*, **125** (8), 082538 (2019).

3. J. Li, G. Miao, Y. Zeng, Z. Zhang, D. Li, H. Song, H. Jiang, Y. Chen, X. Suna, and Z. Lia, *Cryst. Eng. Comm.*, **19**, 88 (2017).

4. D. Stange, N. von den Driesch, T. Zabel, F. Armand-Pilon, D. Rainko, B. Marzban, P. Zaumseil, J.-M. Hartmann, Z. Ikonic, G. Capellini, S. Mantl, H. Sigg, J. Witzens, D. Grützmacher, and D. Buca, *ACS Photonics*, **5** (11), 4628 (2018).

5. F. T. Armand Pilon, A. Lyasota, Y.-M. Niquet, V. Reboud, V. Calvo, N. Pauc, J. Widiez, C. Bonzon, J. M. Hartmann, A. Chelnokov, J. Faist, and H. Sigg, *Nat Commun*, **10**, 2724 (2019).

6. A. A. Hopgood, *J. Appl. Physics*, **76**, 4068 (1994).

7. X. W. Liu, A. A. Hopgood, B. F. Usher, H. Wang, and N. S. Braithwaite, *J. Appl. Phys.*, **94**, 7496 (2003).

8. X. W. Liu, A. A. Hopgood, B. F. Usher, H. Wang, and N. S. Braithwaite, *J. Appl. Phys*. **88**, 5975 (2000).

9. J. H. van der Merwe, *J. Electronic Materials*, **20**, 793 (1991).

10. J. W. Matthews and A. E. Blakeslee, *J. Crystal Growth*, **27**, 118 (1974).

11. D. J. Dunstan, P. Kidd, L. K. Howard, and R. H. Dixon, *Appl. Phys. Lett.*, **59**, 3390 (1991).

12. X. W. Liu, A. A. Hopgood, B. F. Usher, H. Wang, and N. S. Braithwaite *Semiconductor Sci. and Tech.* **14**, 1154 (1999).

13. A. Gangopadhyay, A. Maros, N. Faleev, and D. J. Smith, *Acta Materialia*, **162**, 103 (2019).

14. M. de la Mata, C. Magén, P. Caroff, and J. Arbiol, *Nano Letters*, **14** (11), 6614 (2014).

15. B. W. Dodson and J. Y. Tsao, *Appl. Phys. Lett.* **51**, 1325(1987).

16. P. Zaumseil, G. G. Fischer, C. Quick, and A. Misiuk, *Phys. Stat. Sol. (a)* **153**, 401(1996).

17. A. L. Esquivel, W. N. Lin, and D. B. Wittry, *Appl. Phys. Lett.* **22**, 414 (1973).

18. S. Kishino, N. Chinone, H. Nakashima, and R. Ito, *Appl. Phys. Lett.* **29**, 488(1976).

19. K. H. Kuesters, B. C. De Cooman, and C. B. Carter, *Phil. Mag. A* **53** 141 (1986).

20. B. Pichaud, P. Jean, and F. Minari, *Phil. Mag. A* **54**, 479(1986).

21. P. Paufler, P. Rotsch, and G. Wagner, *Phil. Mag. A* **56**, 533 (1987).

22. S. A. Erofeeva, *Phil. Mag. A* **70**, 943(1994).

23. M. Huang, P. Rugheimer, M. G. Lagally, and Feng Liu, *Phys. Rev. B* **72**, 085450 (2005).

24. F. Liu, P. Rugheimer, E. Mateeva, D. E. Savage, and M. G. Lagally, *Nature* **416**, 498 (2002).

25. I. Yonenaga, Y. Ohno, T. Taishi, and Y. Tokumoto, *Physica B: Condensed Matter*, **404**, 4999 (2009).

26. R. Gentle, P. Edwards and W. Bolton, *Mechanical Engineering Systems*, Butterworth-Heinemann (2001).

27. B. Goodno and J. Gere, *Mechanics of Materials*, CL Engineering (2017).

28. B. Pichaud, M. Putero, and N. Burle *J. De Physique IV* **8**, 227 (1998).

29. S. N. G. Chu, A. T. Macrander, K. E. Strege, and W. D. Johnston *J. Appl. Phys.* **57**, 249 (1985).

30. E. Nadgornyi, *Dislocation Dynamics and Mechanical Properties of Crystals*, Pergamon Press (1988).

31. M. Born & K. Huang, Dynamical Theory of Crystal Lattices, 5th edition, Oxford University Press (1998).

32. D. Hull and D. J. Bacon, *Introduction to Dislocations*, 5th Edition, Elsevier (2011).

33. J. W. Matthews, A. E. Blakeslee and S. Mader, *Thin Solid Films*, 33 (2), pp 253-266 (1976).

34. A.P. Sutton and R.W. Balluffi, *Interfaces in Crystalline Materials*, Oxford University Press (2006).

35. J. W. Matthews, in *Dislocations in Solids*, edited by F. R. N. Nabarro, North-Holland Publishing Co., Vol. 2, pp. 461–545 (1979).

36. M. Willander and S.C. Jain, *Silicon-Germanium Strained Layers and Heterostructures* Academic Press (2003).